The Resonant Scattering and Diffraction Beamline P09 at PETRA III

Jörg Strempfer, DESY, Hamburg

- Introduction
- Examples of experiments using resonant scattering
- Beamline characteristics and components
- First results from commissioning
- Summary of beamline features
- Outlook

Experimental floor at Petra III

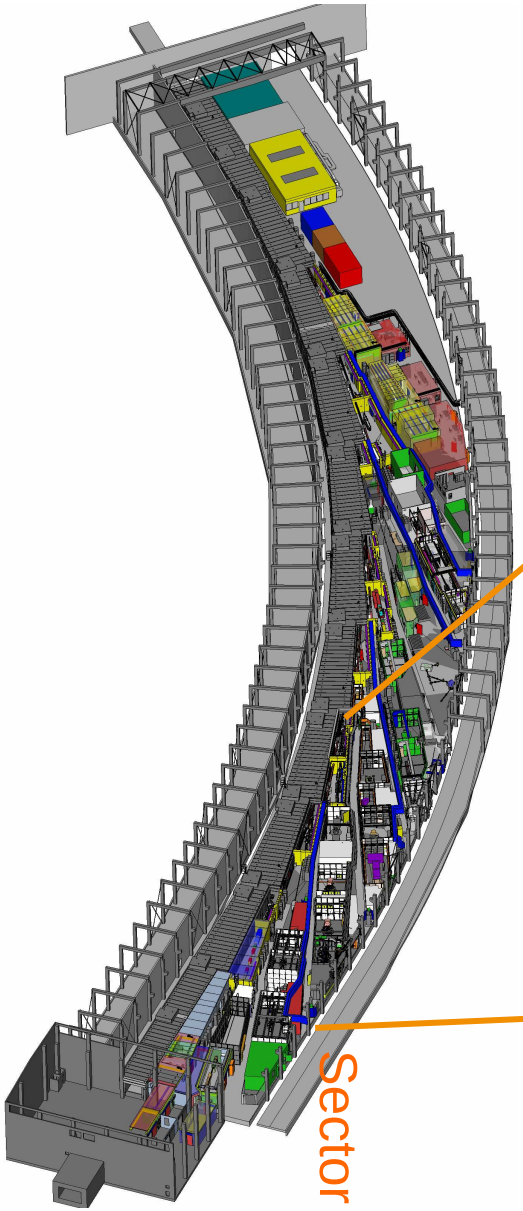

Number	Name	Energy range	Comment	Contact
P01	Dynamics beamline	5 - 40 keV		H. Franz, DESY
P02	Hard X-ray scattering/diffraction	30 - 100 keV	straight	DESY
P03	Micro SAXS/WAXS	8 - 25 keV	down	S. Roth, DESY
P04	Variable Polarization XUV	0.2 - 3.0 keV		J. Viefhaus, DESY
P05	Micro- and nano-tomography / imaging	8 - 25 keV	side	A. Haibel, DESY/GKSS
P06	Micro/nano-spectroscopy / fluorescence	2.4 - 50 keV	straight	G. Falkenberg, DESY
P07	High energy materials science and diffraction	40 - 300 keV		N. Schell, GKSS/DESY
P08	High resolution diffraction	5.4 - 30 keV	top	O. Seeck, DESY
P09	Resonant scattering / diffraction	2.4 - 50 keV	straight	J. Strempfer, DESY
P10	Coherence applications	4 - 25 keV		O. Leupold, DESY
P11	MX-diffraction / biological imaging	8 - 20 keV	side	MPI, HGF, DESY
P12	BioSAXS	4 - 20 keV	straight	M. Rößle, EMBL
P13	Macro molecular crystallography I	5 - 35 keV	side	M. Cianci, EMBL
P14	Macro molecular crystallography II	5 - 35 keV	straight	G. Bourenkov, EMBL

high beta section	142x5 µm
low beta section	35x6 µm

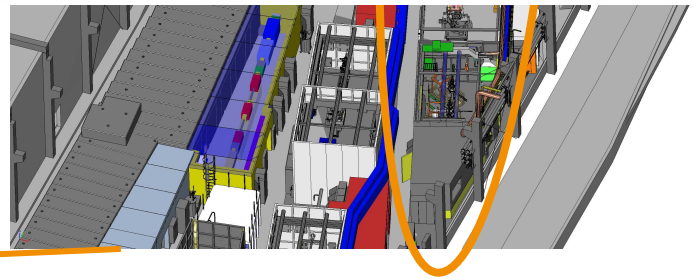

Introduction: Beamlines at sector 6

- High Resolution Diffraction (P08)

- Resonant Scattering and Diffraction (P09)
  - First hutch: high precision diffractometer
  - Second hutch: heavy load diffractometer
  - Third hutch: Hard X-ray Photoelectron Spectroscopy (HAXPES)

Experiments performed at P09:
- Diffraction experiments using special sample environments
- Polarization dependent studies
- Resonant scattering experiments at low temperatures and high fields

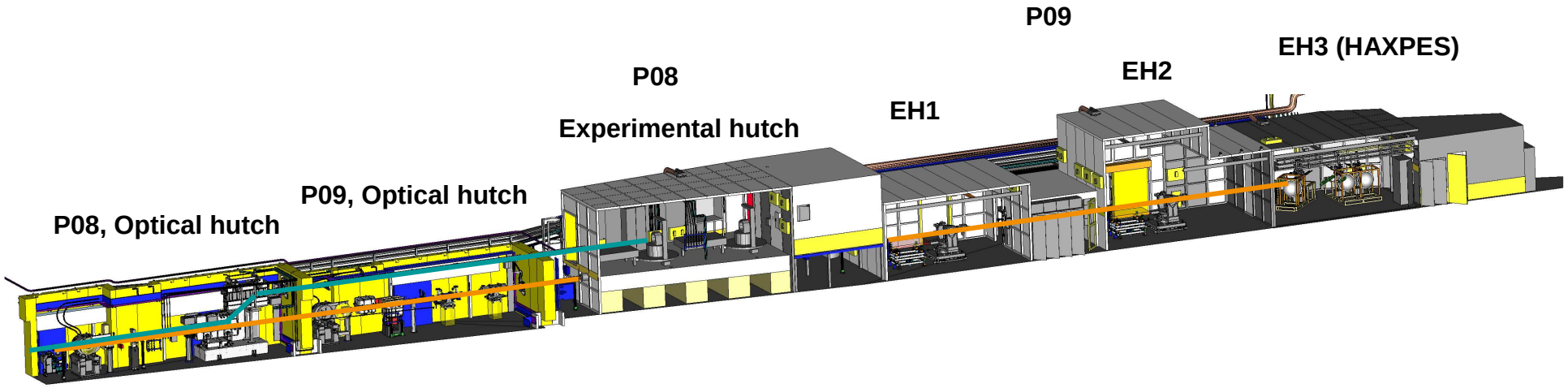

Scattering scheme with polarization analysis

Non-resonant magnetic scattering amplitude [Blume & Gibbs]

$$f^{mag} = -i\frac{\eta\omega}{mc^2}\begin{pmatrix} f^{\sigma\sigma'} & f^{\sigma\pi'} \\ f^{\pi\sigma'} & f^{\pi\pi'} \end{pmatrix}$$

$$= -i\frac{\eta\omega}{mc^2}\begin{pmatrix} S_2 \sin 2\theta & -2\sin^2\theta[\cos\theta(L_1+S_1)-S_3\sin\theta] \\ 2\sin^2\theta[\cos\theta(L_1+S_1)+S_3\sin\theta] & \sin 2\theta[2L_2\sin^2\theta+S_2] \end{pmatrix}$$

Determination of L/S ratio
Magnetic structure determination

Resonant magnetic scattering amplitude (electric dipole transitions) [Hill & McMorrow]

$$f_{E1}^{res-mag} = \begin{pmatrix} f^{\sigma\sigma'} & f^{\sigma\pi'} \\ f^{\pi\sigma'} & f^{\pi\pi'} \end{pmatrix}$$

$$= F^0 - iF^1\begin{pmatrix} 0 & m_1\cos\theta + m_3\sin\theta \\ m_3\sin\theta - m_1\cos\theta & -m_2\sin 2\theta \end{pmatrix}$$

$$+ F^2\begin{pmatrix} m_2^2 & m_2(m_1\sin\theta - m_3\cos\theta) \\ m_2(m_1\sin\theta + m_3\cos\theta) & -\cos^2\theta(m_1^2\tan\theta + m_3^2) \end{pmatrix}$$

Strong intensities due to resonance enhancement
Element sensitivity at absorption edges
Magnetic structure determination

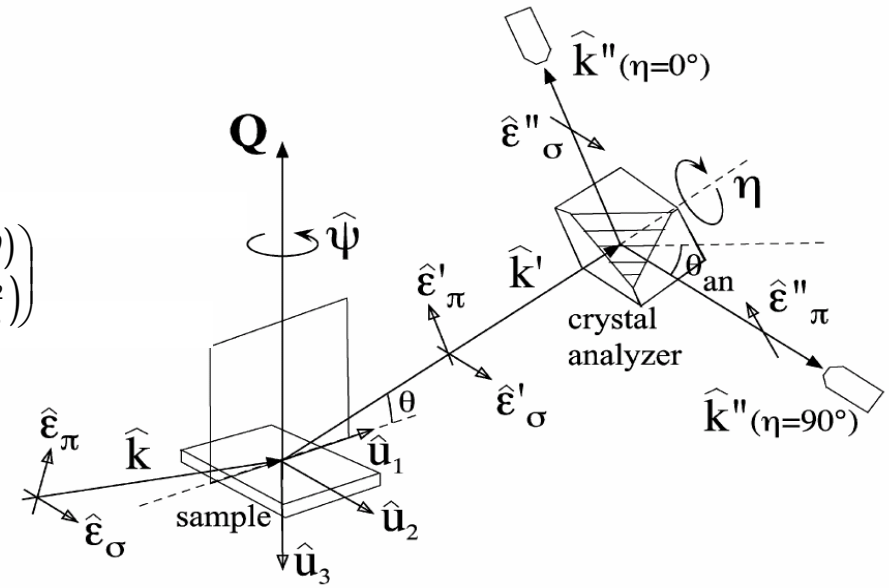

L/S determination

Non-resonant magnetic diffraction from $KCuF_3$

Ciaruffo et al., PRB 65, 174455 (2002)

Magnetic moment in basal-plane (S_3=0)

L and S collinear: $S_1 = S\cos\alpha$

$S_2 = S\sin\alpha$

Scattering amplitude:

$$\begin{pmatrix} f_{\sigma\sigma'} \\ f_{\sigma\pi'} \end{pmatrix} = \begin{pmatrix} S\sin\alpha\sin 2\theta \\ -2(L+S)\cos\alpha\cos\theta\sin^2\theta \end{pmatrix}$$

$$\frac{L(Q)}{S(Q)} = \frac{\tan\alpha}{\sin\theta}\sqrt{\frac{I_{\sigma\pi'}}{I_{\sigma\sigma'}}}$$

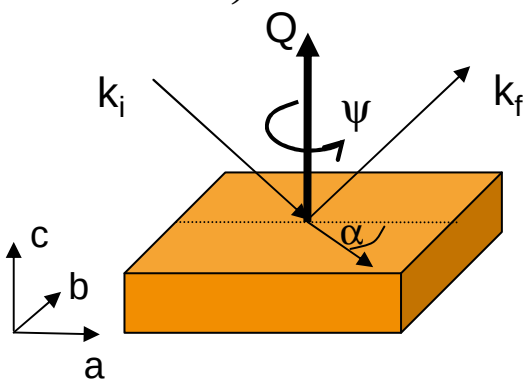

Magnetic moment || (110)

→ L/S=0.29(5)

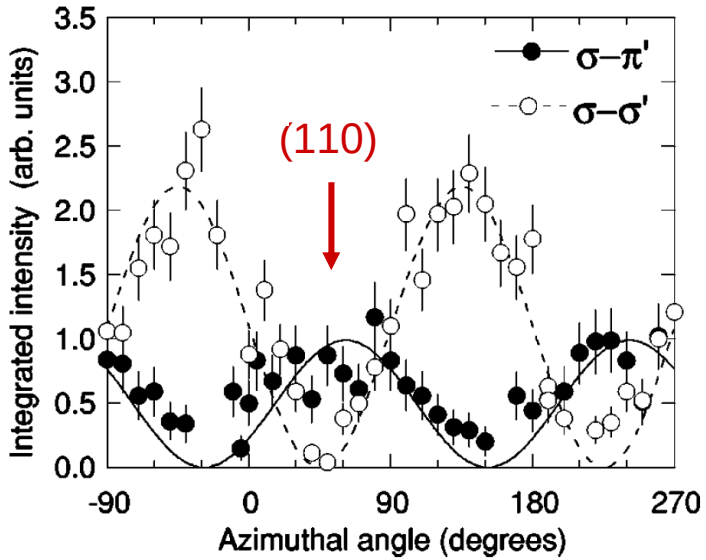

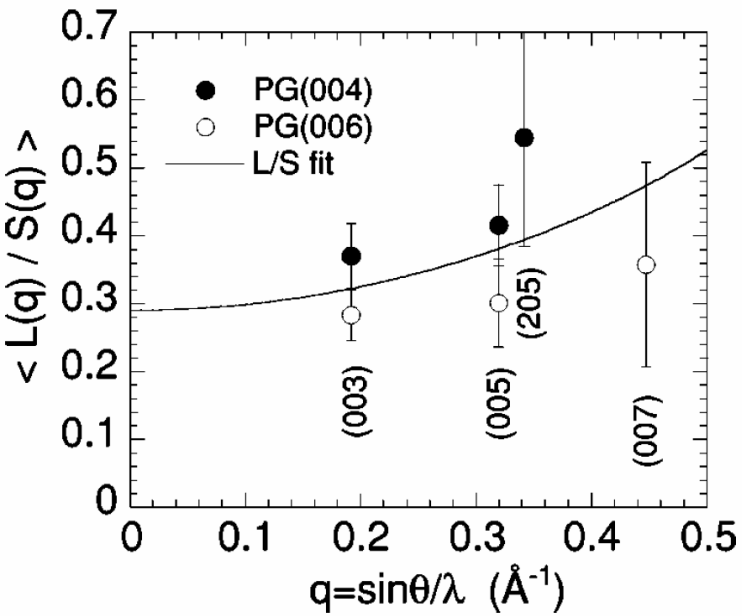

Polarization dependent studies on resonance

Resonant magnetic studies in $TbMn_2O_5$

Johnson et al. PRB 78, 104407 (2008)

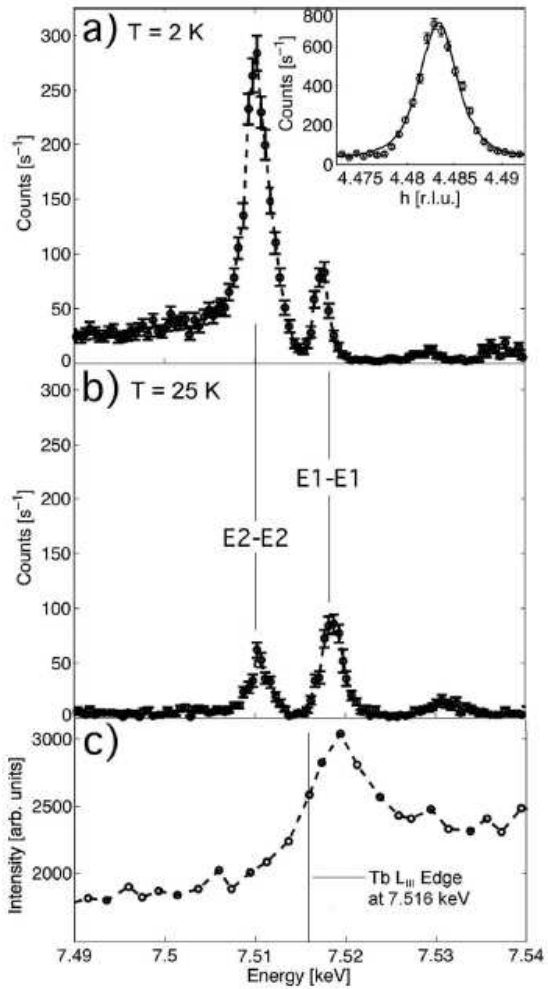

Properties of $TbMn_2O_5$:

- low temperatures: Mn^{3+}, Mn^{4+}, Tb^{3+} order coexistent wave vector (δ, 0, τ)
- T_N < 43 K: incommensurate ICM2 phase
- T_{FE} = 38 K: onset of ferroelectric order P||b
- 33 K > T > 24 K: commensurate (CM) phase
- T < 24 K: incommensurate ICM1 phase

Tb L_{III} resonance: 2p → 5d

Investigation of dipolar (E1-E1) and quadrupolar (E2-E2) resonances

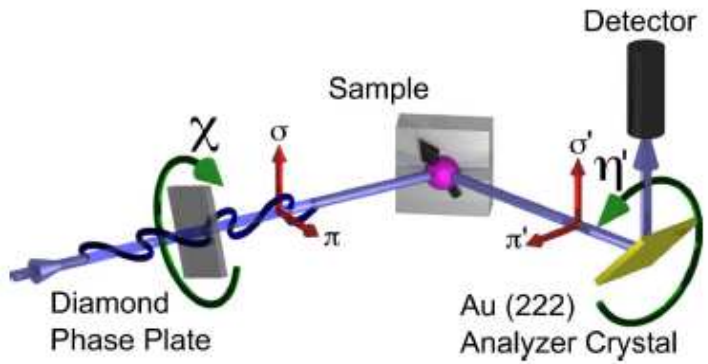

Polarization dependent studies on resonance

Resonant magnetic studies in $TbMn_2O_5$

Determination of magnetic order

Johnson et al. PRB 78, 104407 (2008)

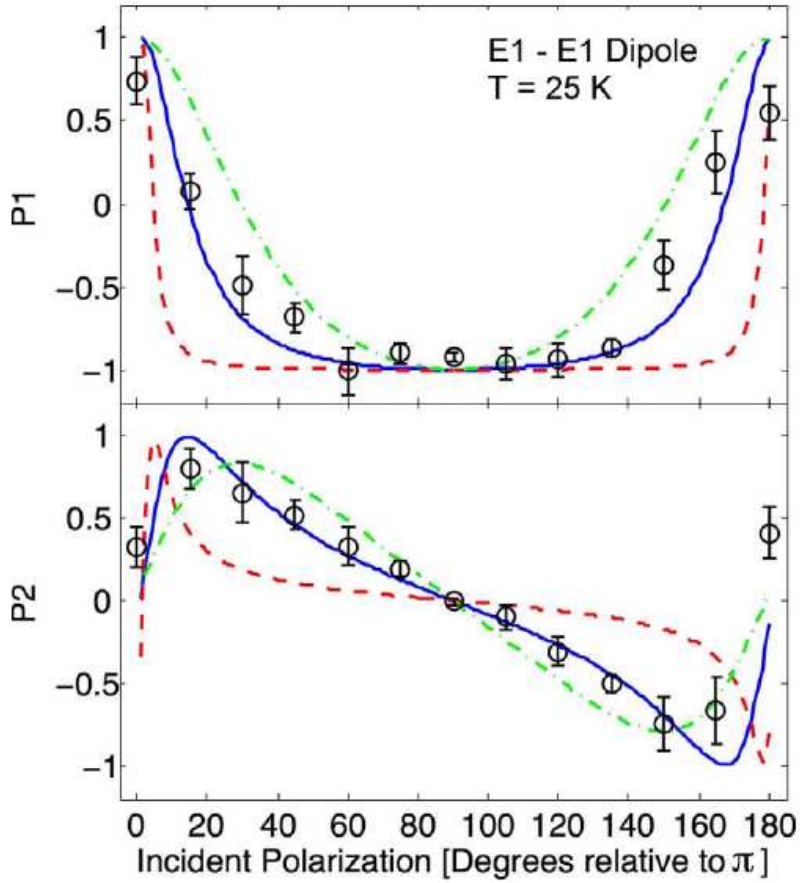

Poincaré-Stokes parameters:

$$P_1 = (I_{\sigma'} - I_{\pi'})/(I_{\sigma'} + I_{\pi'})$$
$$P_2 = (I_{+45^{o'}} - I_{-45^{o'}})/(I_{+45^{o'}} + I_{-45^{o'}})$$
$$P_C = (I_{R'} - I_{L'})/(I_{R'} + I_{L'})$$

→ Terbium magnetism result of interaction with Mn^{4+} magnetic moment

Blake et al. PRB 71, 214402 (2005)

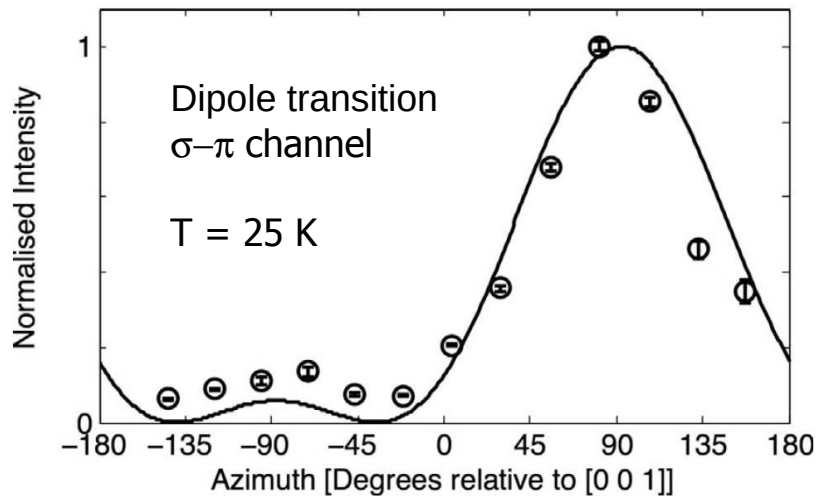

Resonant magnetic scattering

L-edges of $Ca_3Ru_2O_7$ at 2.838 and 2.968 keV

Bohnenbuck, Zegkinoglou, Strempfer et al., PRB, 77, 224412 (2008)

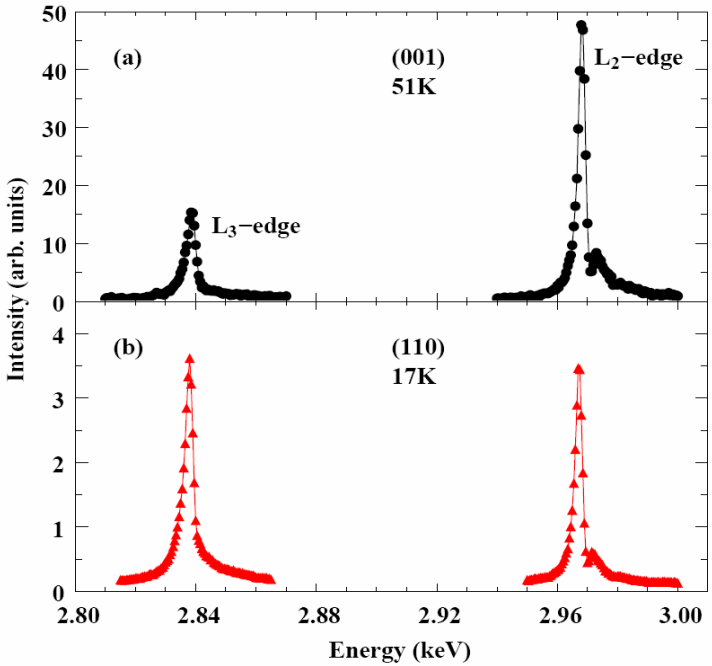

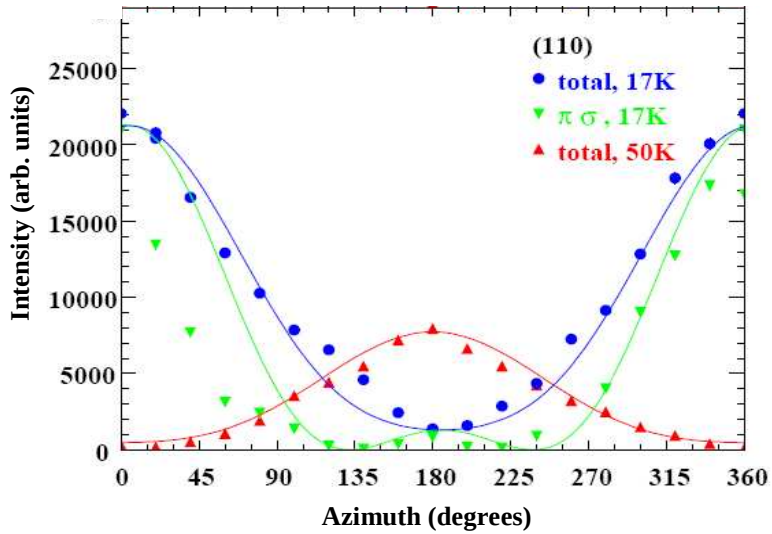

Magnetization flop at T_{MI}=48 K: m||b → m||a

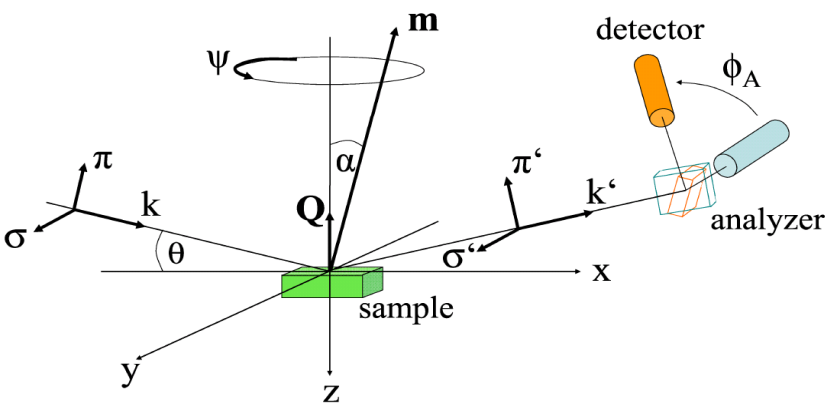

Important information on moment orientation or orbital occupancies from azimuthal dependences

Azimuthal rotation of sample *equivalent* to rotation of plane of linear polarization

→ investigation of single grains without ‚grain hopping'

Azimuthal dependences on real samples

Problem

- Grain hopping on multi grain samples
- Screening of domains in irregular samples

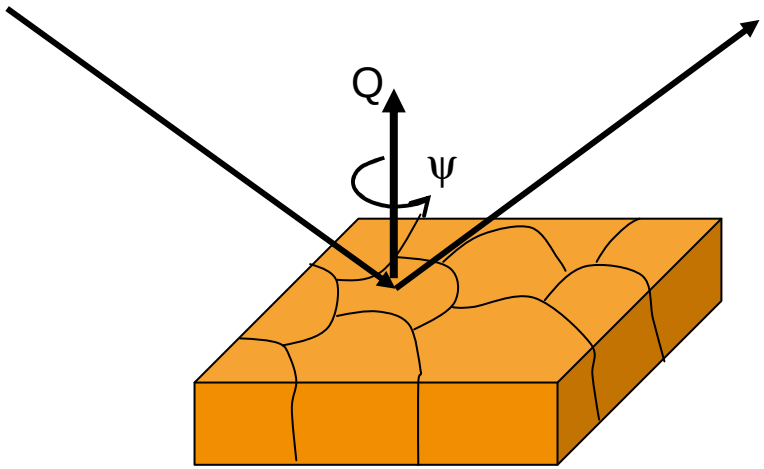

Solution

- Substitution of azimuthal dependence of intensity by rotation of polarization
- Small beam focus
- Measurement of Stokes parameters using full polarization analysis

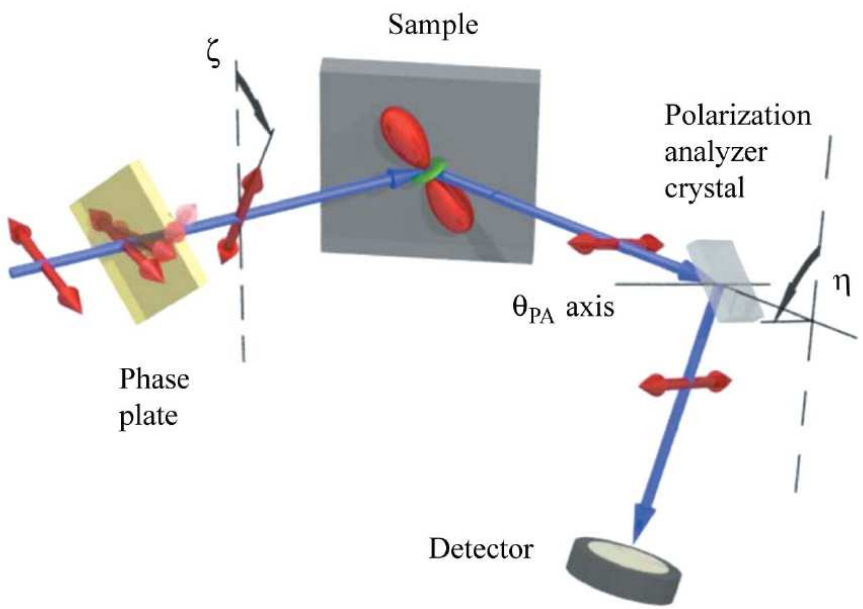

High magnetic field measurements

Investigation of multiferroic $TbMnO_3$ at polarization flop transition

Strempfer et al., PRB, 78, 024429 (2008)

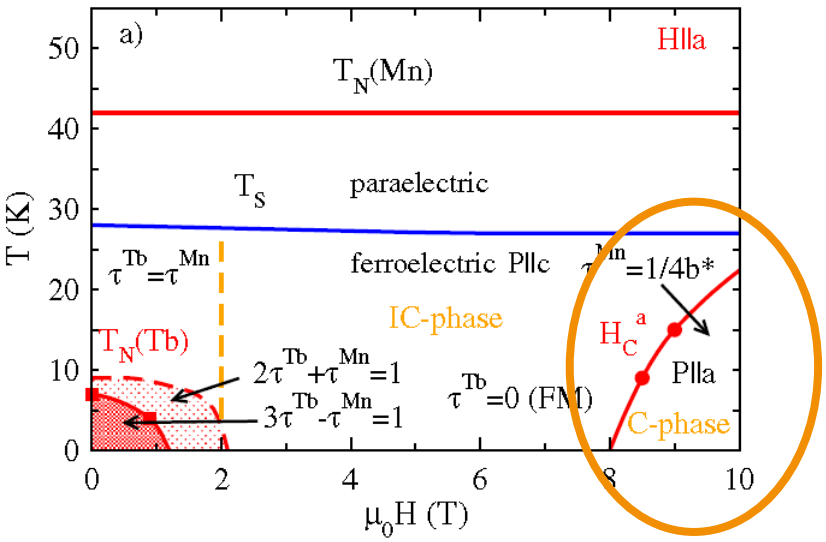

Resonant magnetic scattering with azimuthal dependence at H_C

→ Direct observation of magnetic moment flop from *ac*-plane into *ab*-plane driving polarization flop *P*||*c* → *P*||*a*

$T_S < T < T_N$=42 K

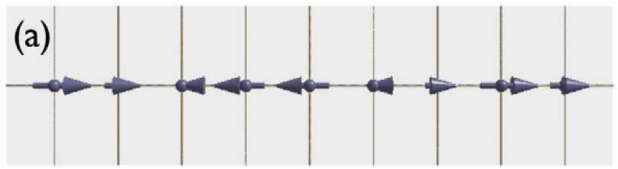

$T < T_S$=28 K

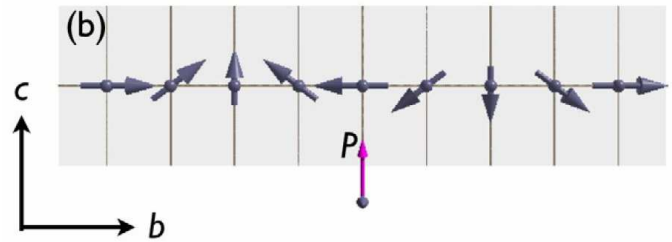

Magnetic excitations

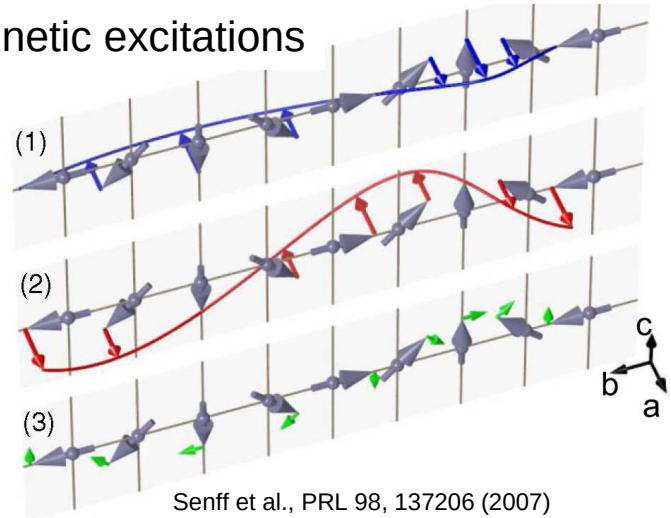

Senff et al., PRL 98, 137206 (2007)

Absorption edges

3d transition metals:
Cr, Mn, … K-edges

4d transition metals
Mo,.., Ru ,… L-edges, K-edges

5d transition metals
…, Re, Os, Ir, … L-edges, M-edges

Rare earths (4f-metals)
Eu, Gd, Tb, … L-edges

Within energy range 2.4 – 24 keV almost all relevant transition metal and rare earth absorption edges are accessible

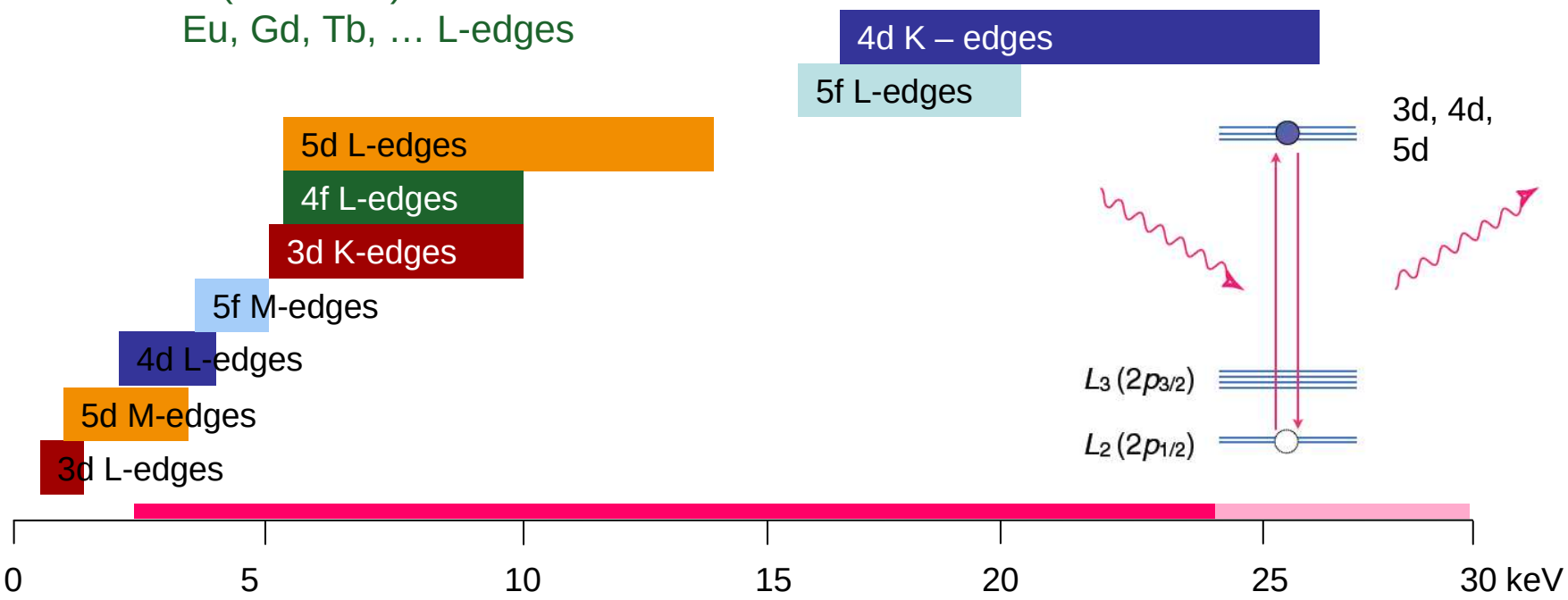

Requirements for resonant scattering and diffraction beamline

- Small beam sizes: routinely 145 x 45 μm^2

  microfocus: 7 x 4 μm^2
- Variable linear and circular polarization
- Efficient higher harmonic suppression in energy range 2.4 – 24 keV
- Custom design Psi diffractometer
  → allow large θ-values
  → quasi simultaneous use of point and area detectors
- Windowless sample environment / in vacuum beam path
- High magnetic fields

Optical beamline components

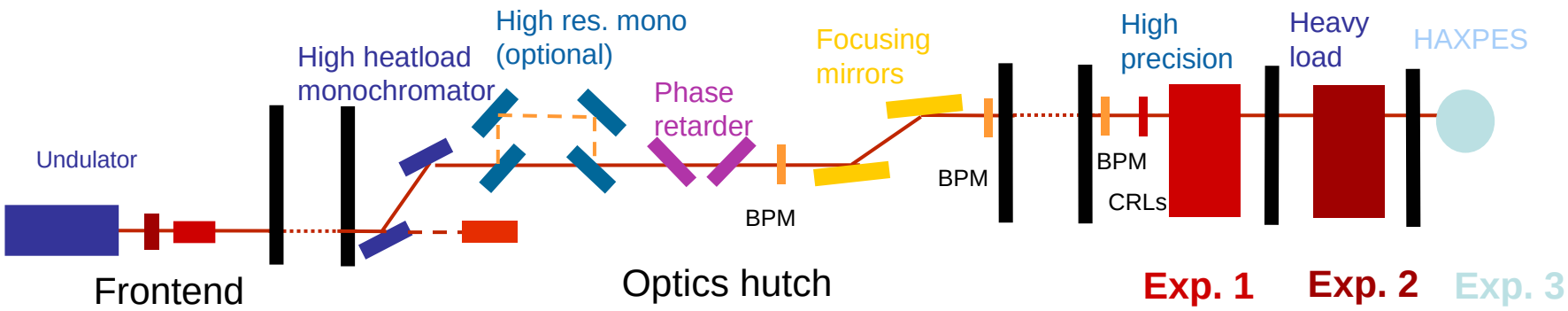

- High-Heatload LN_2 cooled monochromator Si(111)/Si(311)
- High resolution monochromator (HAXPES)
- Phase plates
- Mirrors

- Compound refractive lenses

Principle of phase retardation

Principle: X-ray phase plates based on birefrigence near Bragg-reflection
→ **use of forward diffracted beam**

Phase difference between transmitted electric field perpendicular (σ) and parallel (π) to diffraction plane:

$$\Delta\Phi = -\frac{\pi}{2}\frac{r_e^2\lambda^3\,\mathrm{Re}\left[F_h F_h^-\right]\sin(2\theta)t}{\left[\pi V\right]^2\Delta\Theta} \sim \frac{t}{\Delta\Theta}$$

Effective thickness of crystal

Angular offset from Bragg reflection

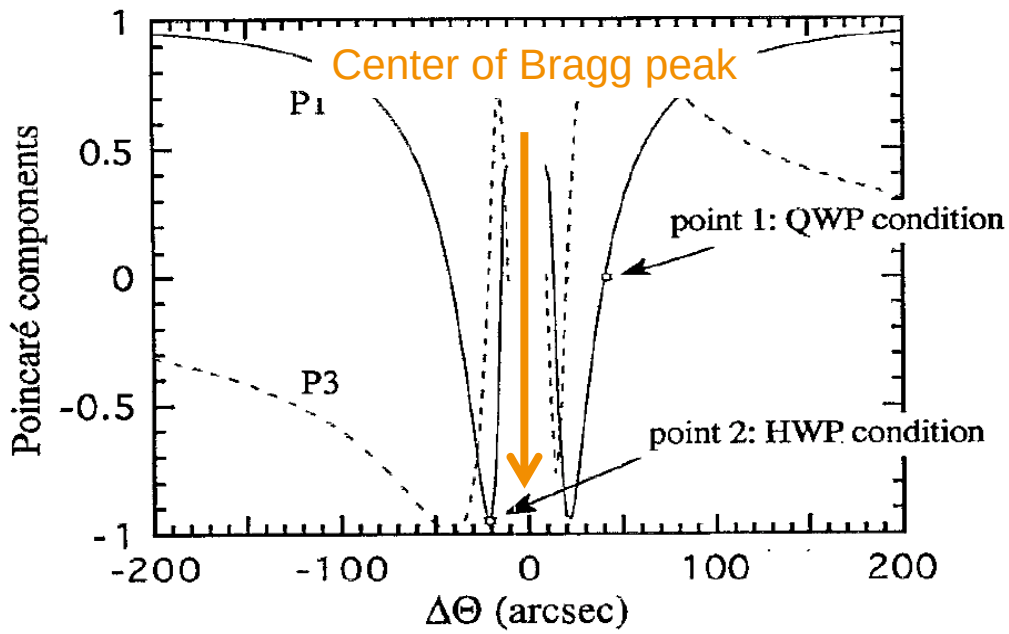

C. Giles et al. Rev. Sci. Instrum. 66, 1519 (1995)

Phase retarder at P09

Diamond phase plates useable for E > 3.5 keV

Quarter wave plate condition (circular polarization):

→ Fast switching between left and right circular polarization

→ Compensation of intensity differences by using 2 phase plates in series

Lang et al., APS Annual Report 2005

Half wave plate condition (linear polarization):

→ Continuous rotation of plane of linear polarization

Giles et al., Rev. Sci. Instrum. 66 (1995), 1518

→ Use of 2 phase plates in series for efficient porarization change

Scagnoli et al. J. Synchrotron Rad. 16 (2009), 778

Rotation of linear polarization, $\Delta\varphi = \pi$:

$$P_1' = 1 - 2\sin^2(2\chi)$$

$$P_2' = \sin(4\chi)$$

$$P_3' = 0$$

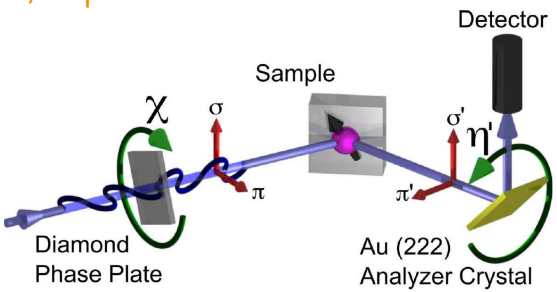

➔ Rotation by angle $\zeta = 2\chi$

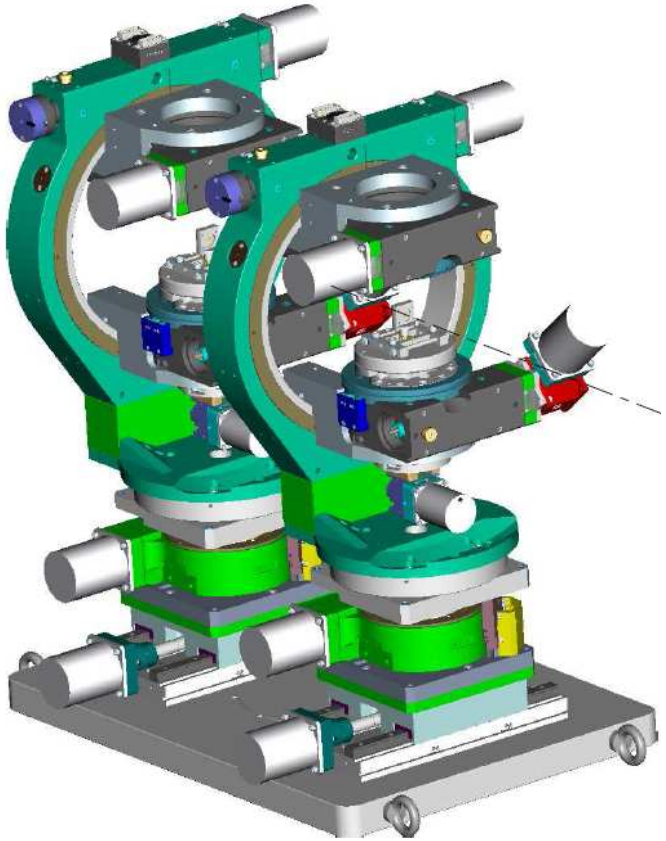

Test of phase plates on diffractometer in EH1

E = 7.828 keV

Diamond (111) reflection with 300 µm diamond plate at sample position

Use of PG(006) as analyzer

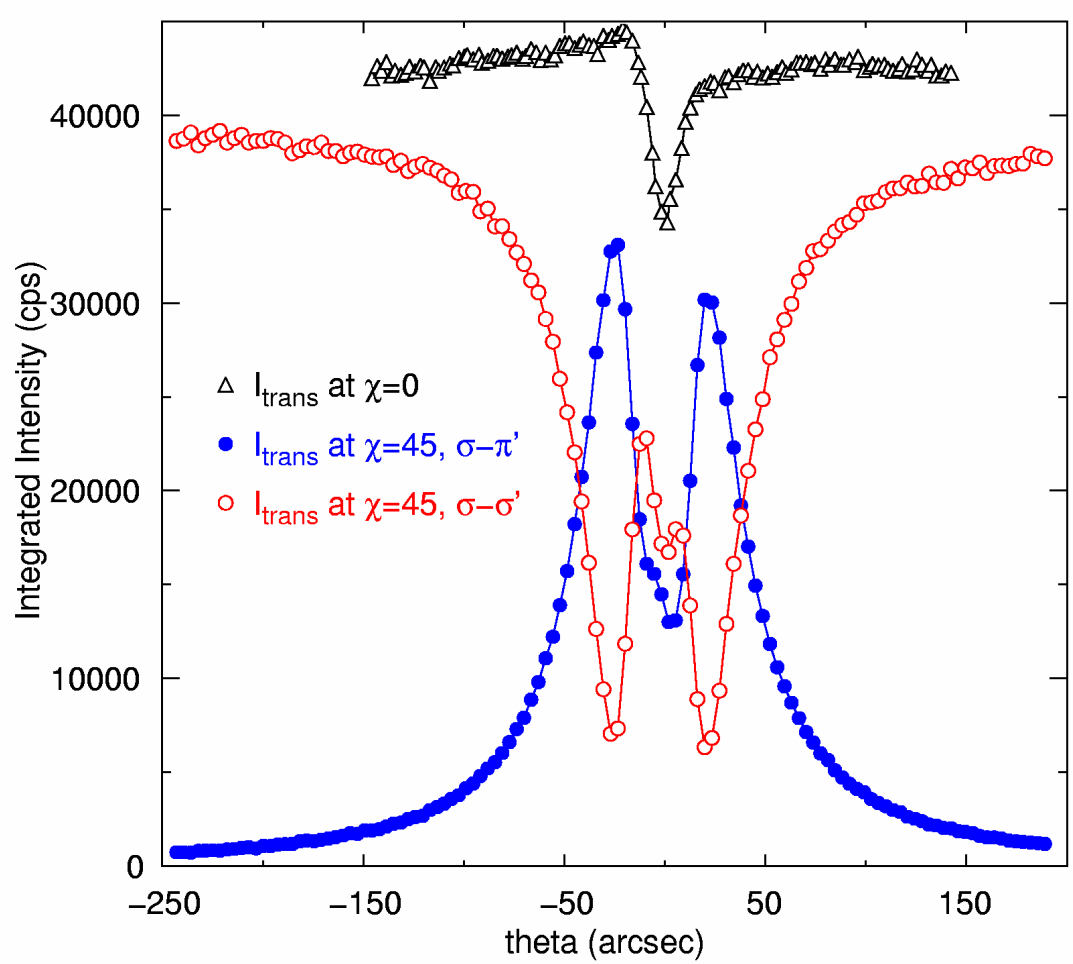

Focusing mirrors

Two 1m long quartz mirrors with partial Pd-coating

Sagittal focusing with fixed cylinders (radius r)

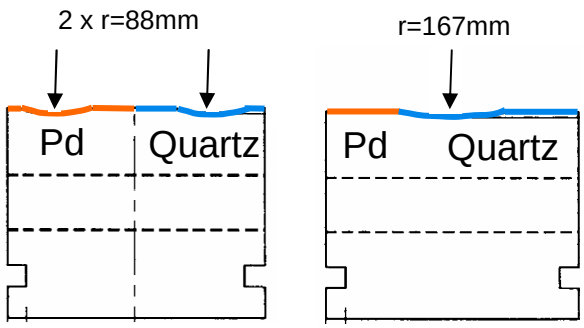

Meridional focusing using variable bender (radius R)

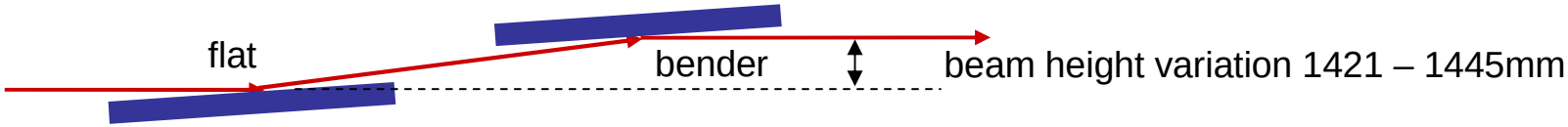

First experimental hutch
Cut offs: 5, 11, 24 keV

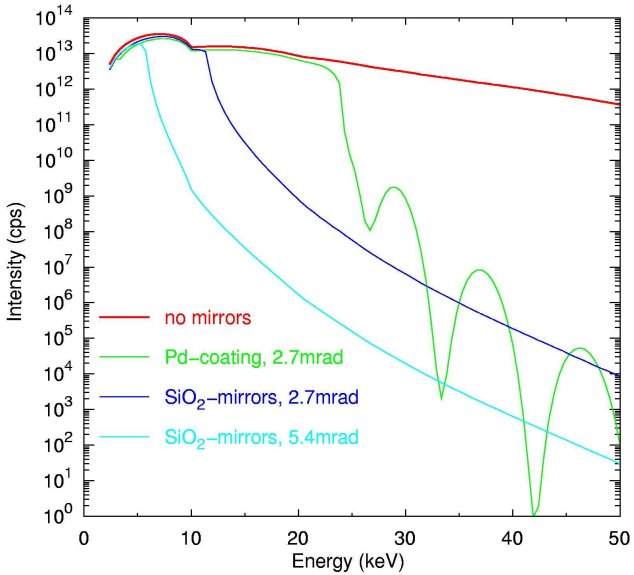

Second experimental hutch
Cut offs: 7, 15, 24 (32) keV

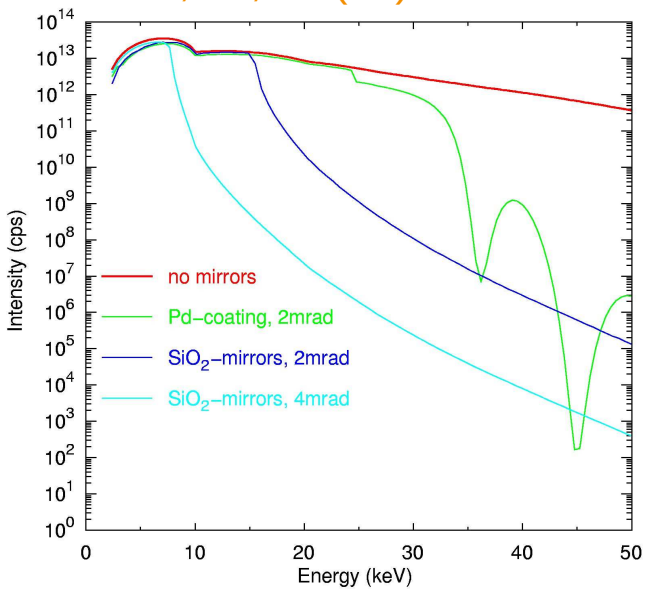

Unfocused / focused beam (ray tracing)

Photon energy 8 keV

76 m | *88 m*

unfocused

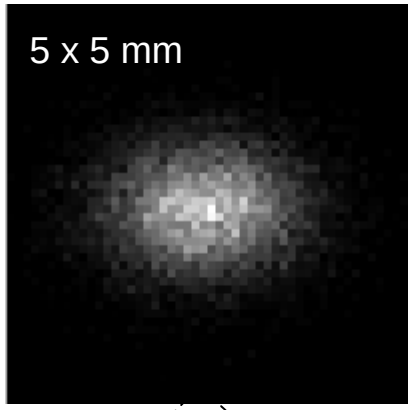

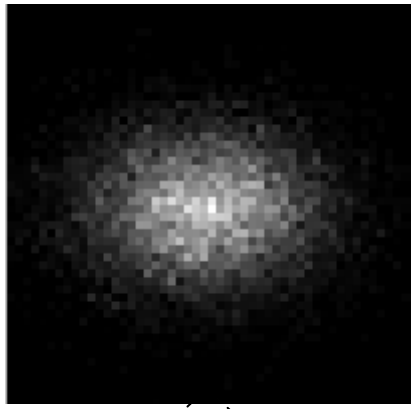

1.7 x1.2 mm^2 (FWHM)

2 x 1.4 mm^2 (FWHM)

focused

r=0.088 m, R=11400 m and α=2.7 mrad

r=0.088 m, R=20900 m and α=2 mrad

145 x 11 μm^2

190 x 12 μm^2

with slope error 0.3 μrad (rms)

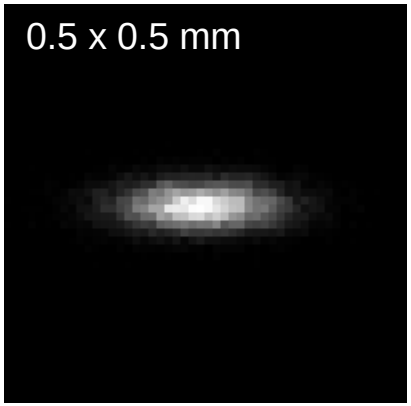

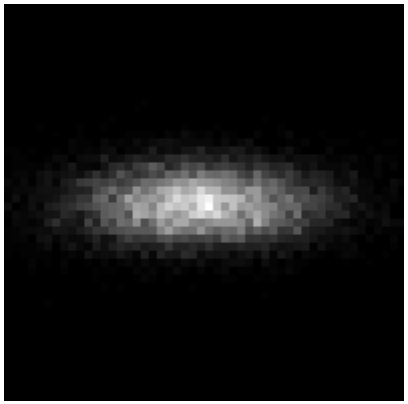

145 x 45 μm^2

200 x 70 μm^2

Beamline components in EH1

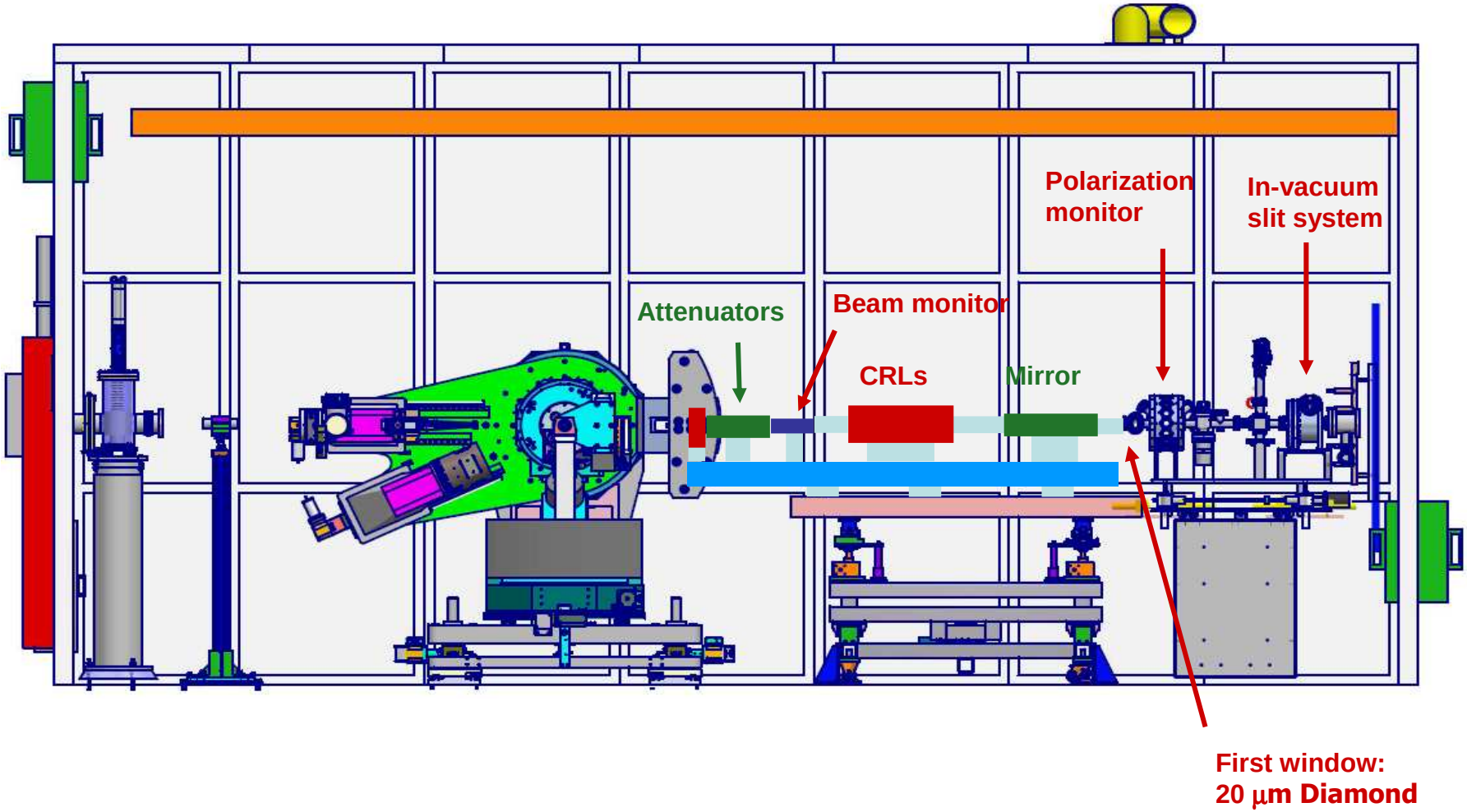

Polarization analysis

Photo-ionization of gas target / angle resolved PES

designed for XUV-beamline (UniHH, PTB and FHI) for < 3keV region

might be expanded towards energies of 15 - 20 keV using Kr or Xe gas

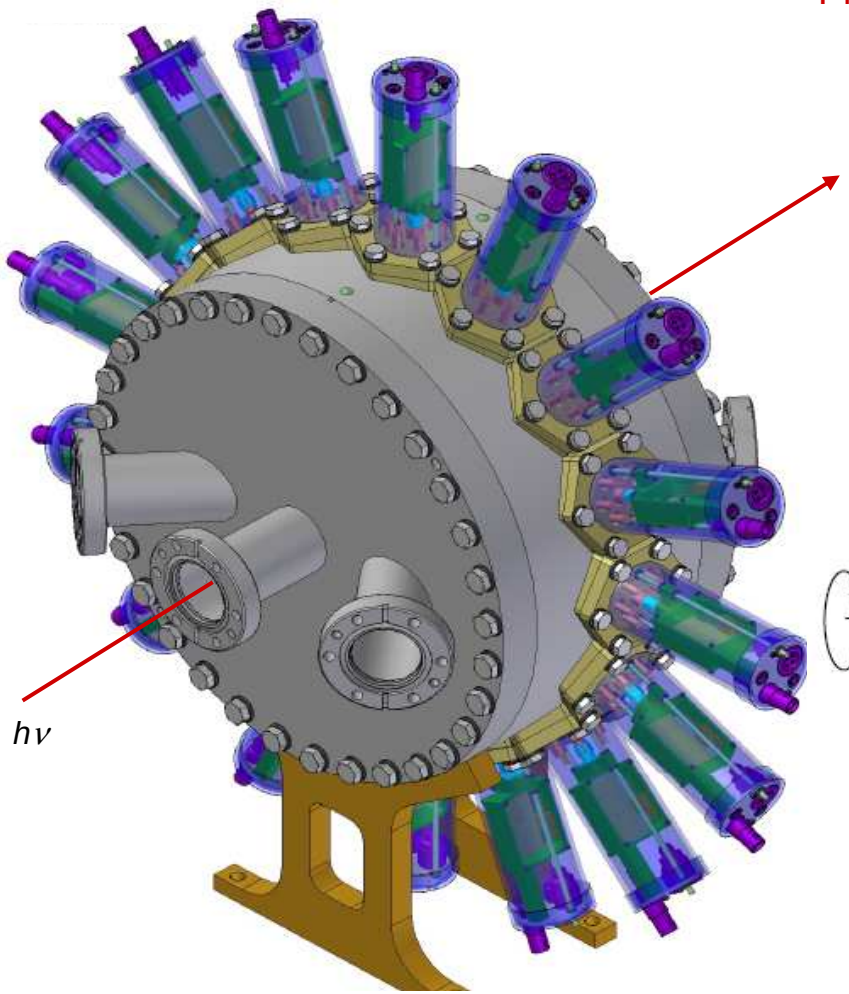

Principle:

- Measurement of angular distribution of photoelectrons.
- Comparision with database gives exact polarization

$$\frac{d\sigma}{d\Omega} = \frac{\sigma}{4\pi}\left(1+\frac{\beta}{4}\left(1+3P_1\cos(2(\Theta-\lambda))\right)\right)$$

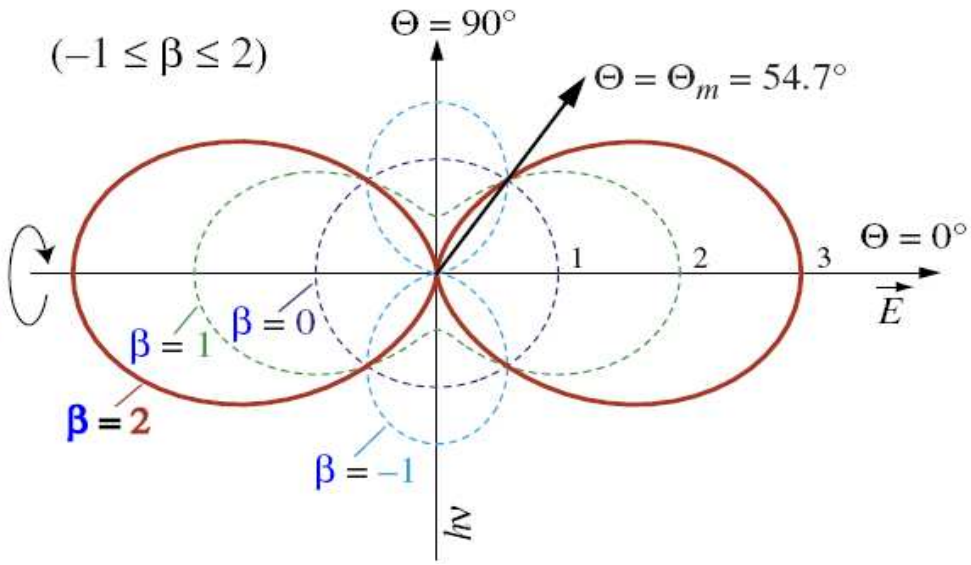

Beam monitor / Attenuator / CRLs

Beam monitor with different foils

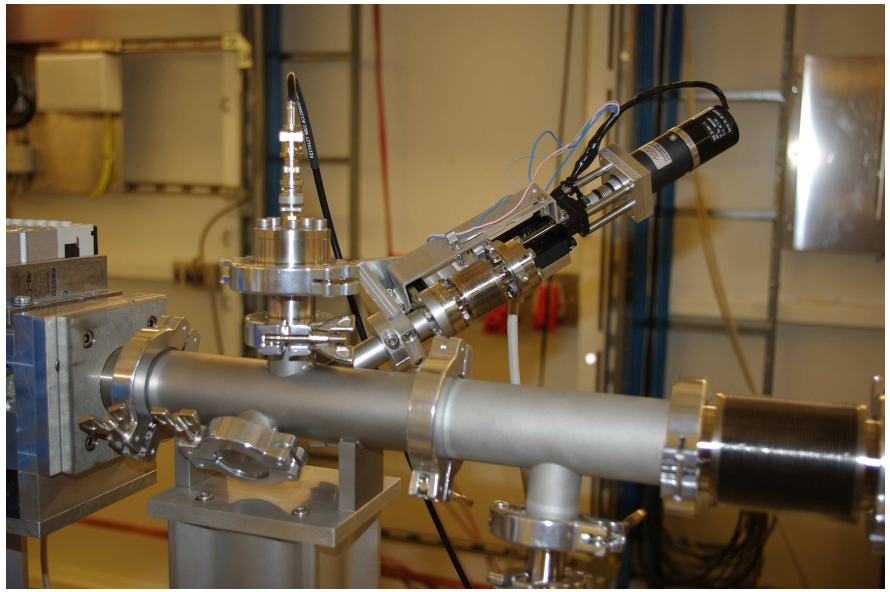

In vacuum attenuator
for 2.4 – 30 keV energy range (12 positions)

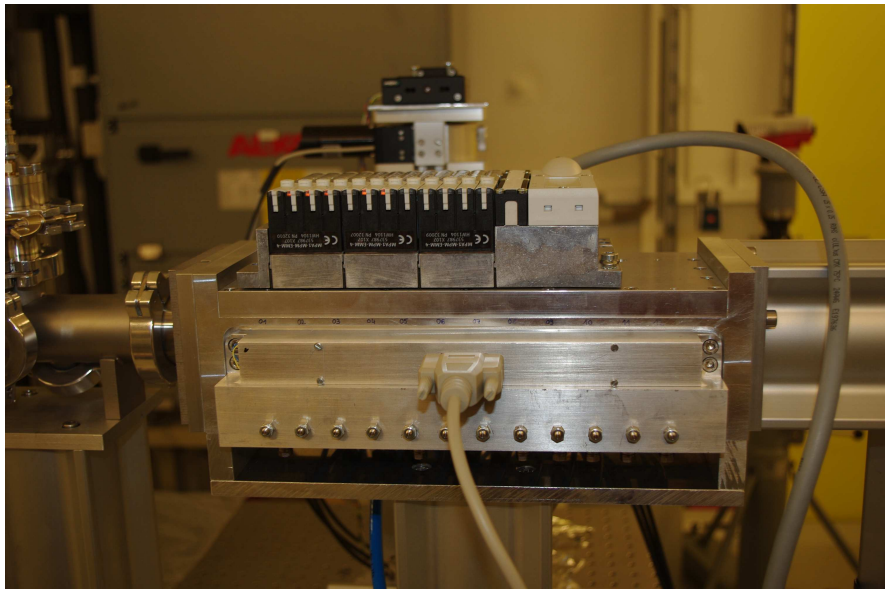

Beam re-focusing using
compound Refractive Lenses

- Beam collimation using with mirrors
- re-focusing with lenses 2 m
  in front of sample

33 lenses with 0.6 mm radius at 10 keV
→ beam size at sample position: 7 x 4 μm^2

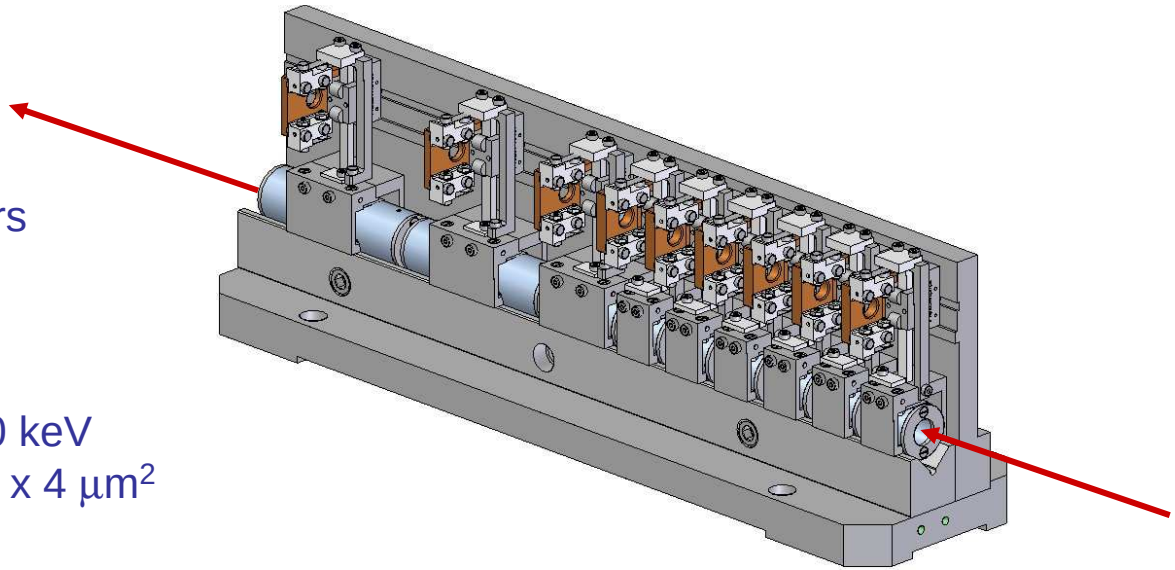

Psi-Diffractometer

- High precision diffractometer with open χ-circle: χ-range ±90° (normally)
  ±45° (with cryostat)
- Spheres of confusion (design):
  - θ-circle: < 60 µm (20 µm)
  - χ-circle: < 20 µm (20 µm)
- Motorized cryostat holder
- Simultaneous use of CCD and point detector
- Windowless beam path up to detector

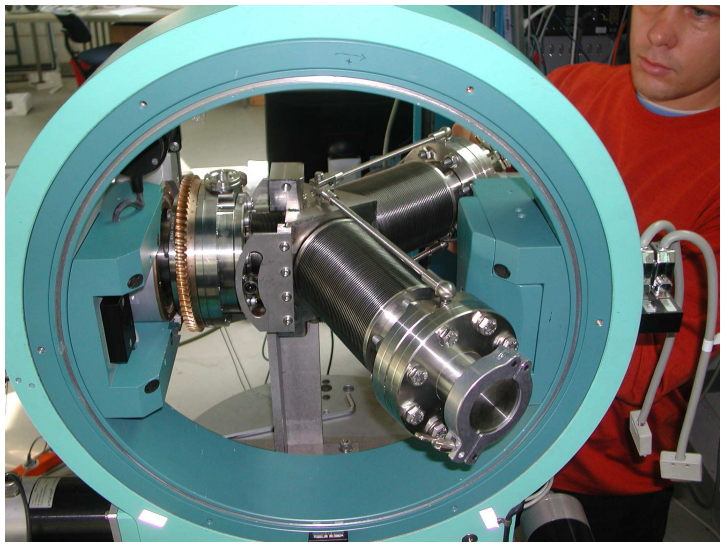

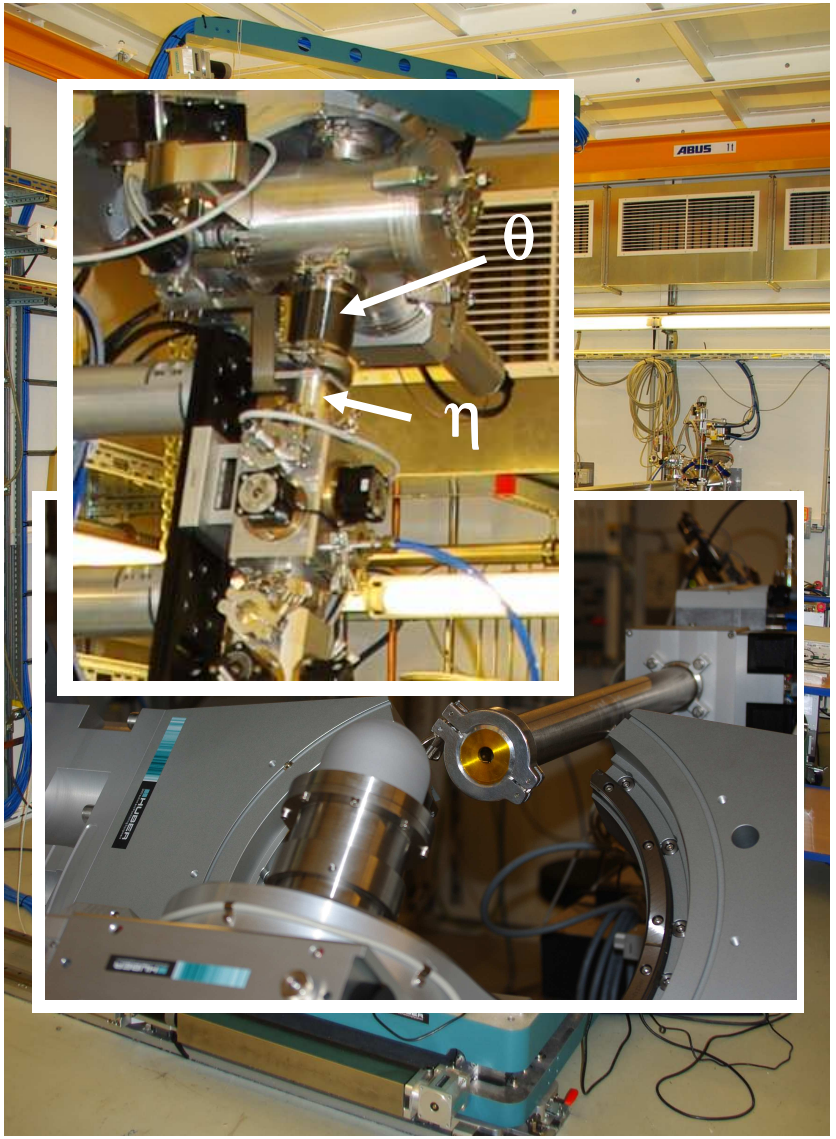

EH2: Heavy load diffractometer: Horizontal Psi-geometry

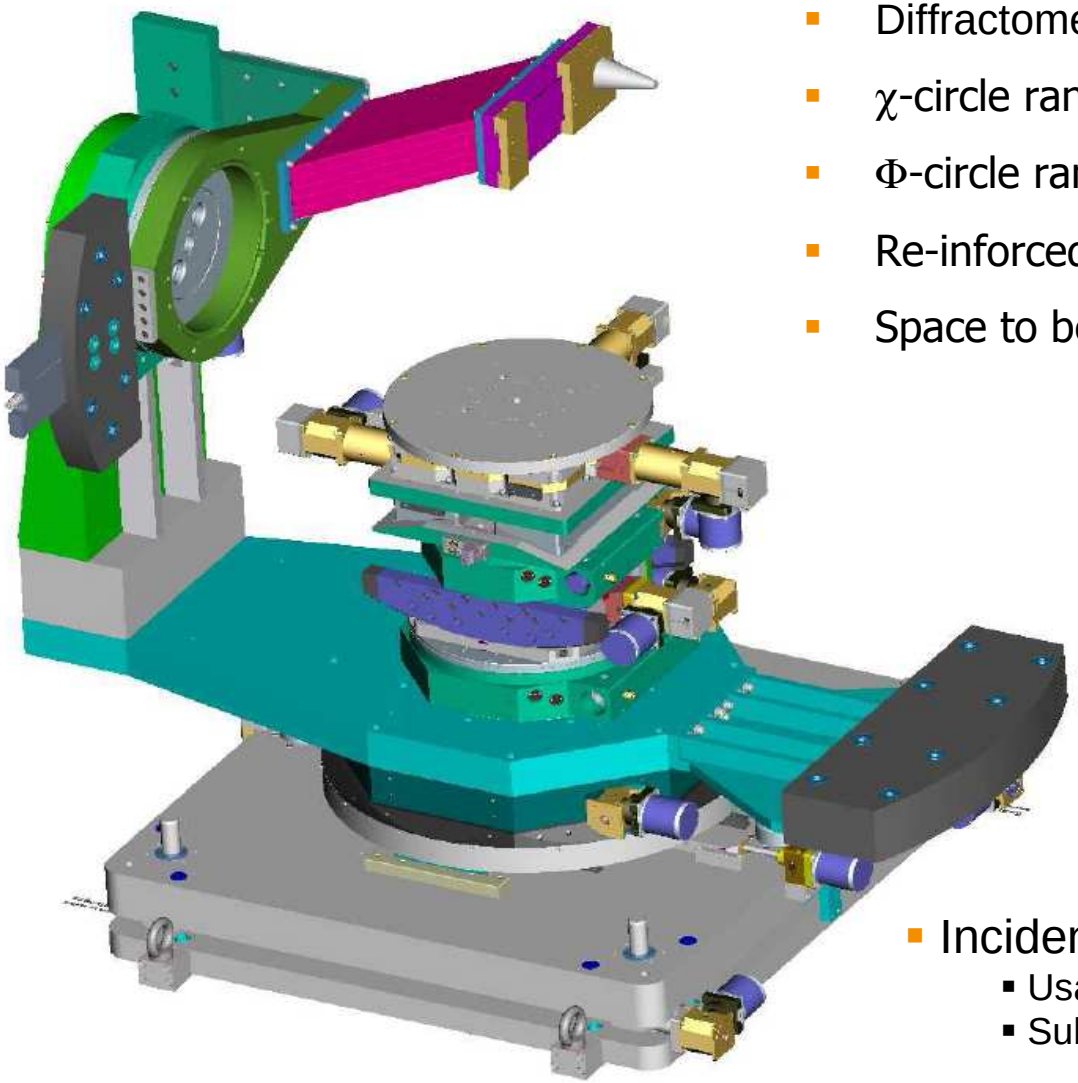

- Diffractometer load capacity: 650 kg
- χ-circle range: +/- 7 deg
- Φ-circle range: +/-180 deg
- Re-inforced 2theta arm
- Space to beam above upper stage: 250 mm

- Incident variable polarization
  - Usage of polarization monitor in first hutch
  - Substitution of azimuthal rotation
- Polarization analysis

14 T cryomagnet fom Cryogenic

- 14 T split coil superconducting magnet
- Vertical field
- Maximum horizontal opening angle

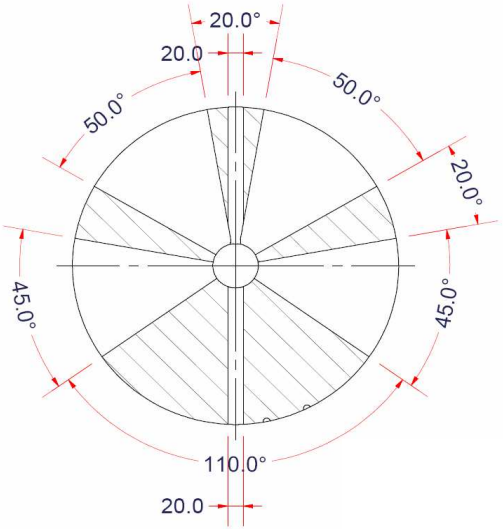

- Beryllium X-ray windows
- Including He^3-refrigerator for temperatures down to 500 mK
- Standard temperature range: 1.8 K – 300 K

First design drawing from Cryogenic

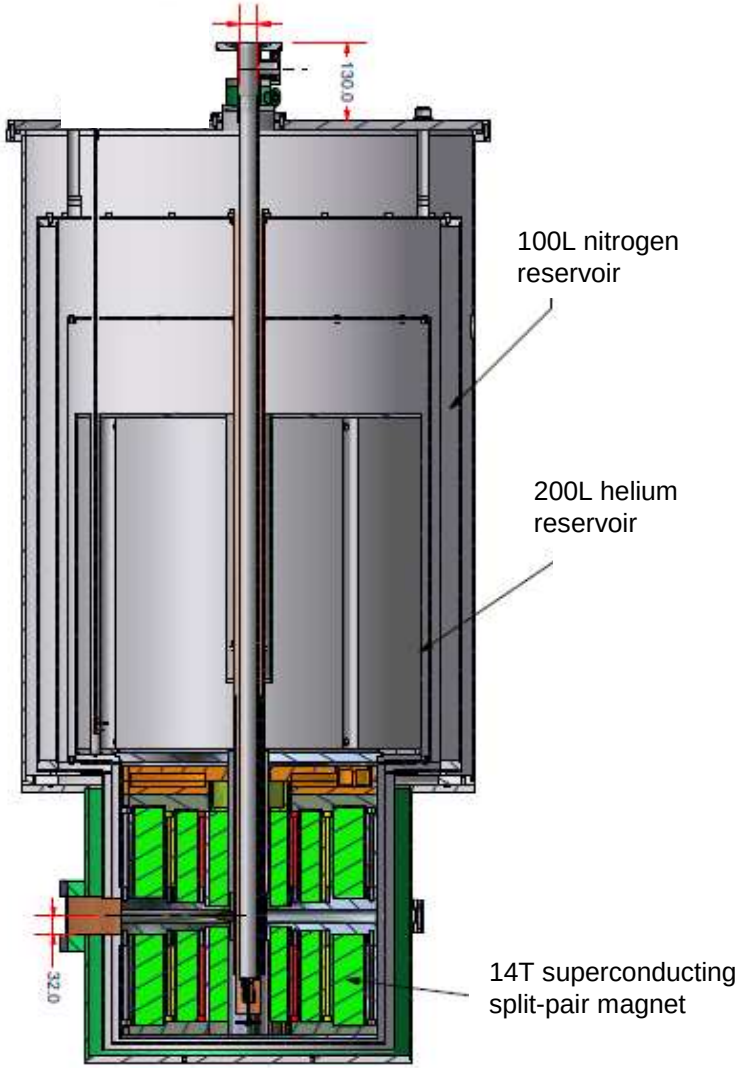

PETRA III top up operation

PETRA Energy: 6.084 GeV Lifetime: 10.00 h Current: 59.45 mA

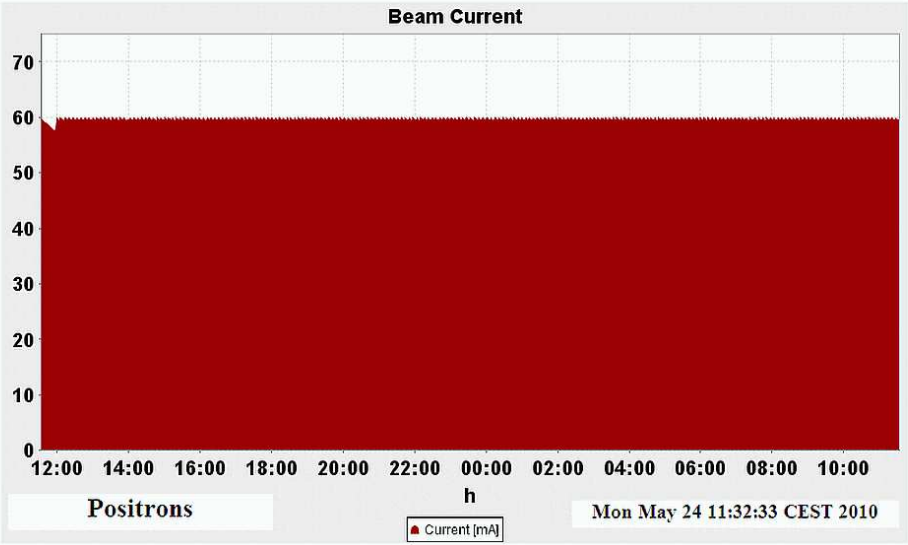

Und.	Gap [mm]	Status
PU01	100.60	
PU03	11.26	
PU04	147.00	
PU05	205.00	
PU06	206.00	
PU07	193.63	
PU08	18.49	
PU09	11.57	
PU10	16.23	
PU12	212.00	

Number of Bunches: 70 Mean Vacuum Pressure: 1.142E-08 mbar

Orbit Control: On Top-Up Operation: 0.06 mA (RMS)

User Operations->Experiments

First experiments in EH1

Energy scan at Cu K_α absorption edge

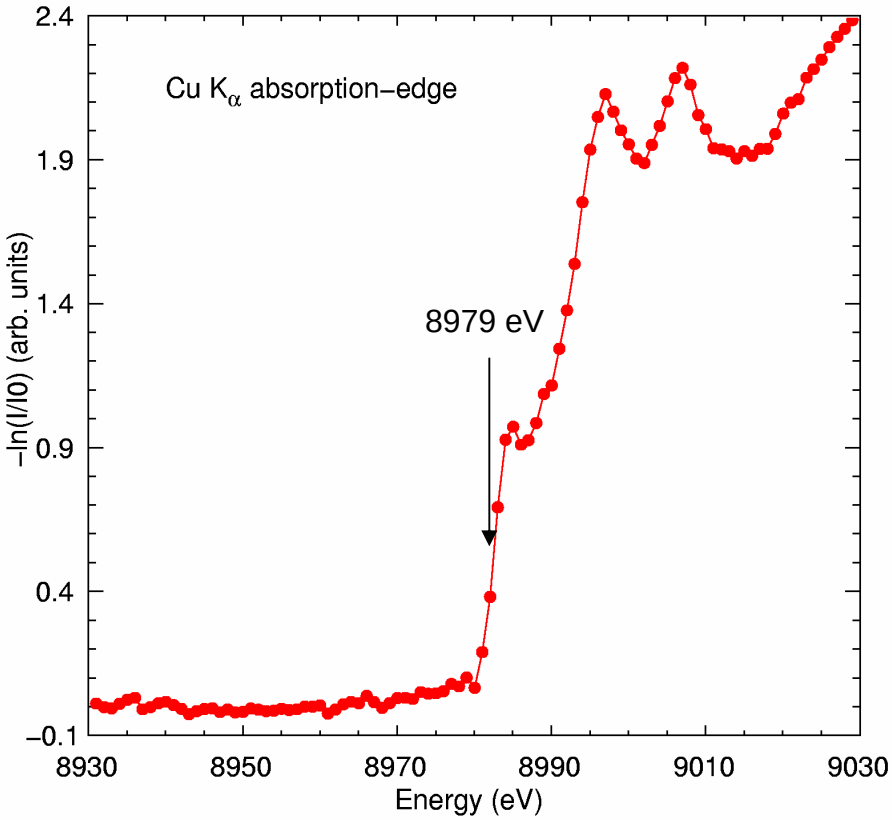

Energy calibration of Monochromator by scanning through absorption edges

Resonant magnetic scattering from $TbMnO_3$

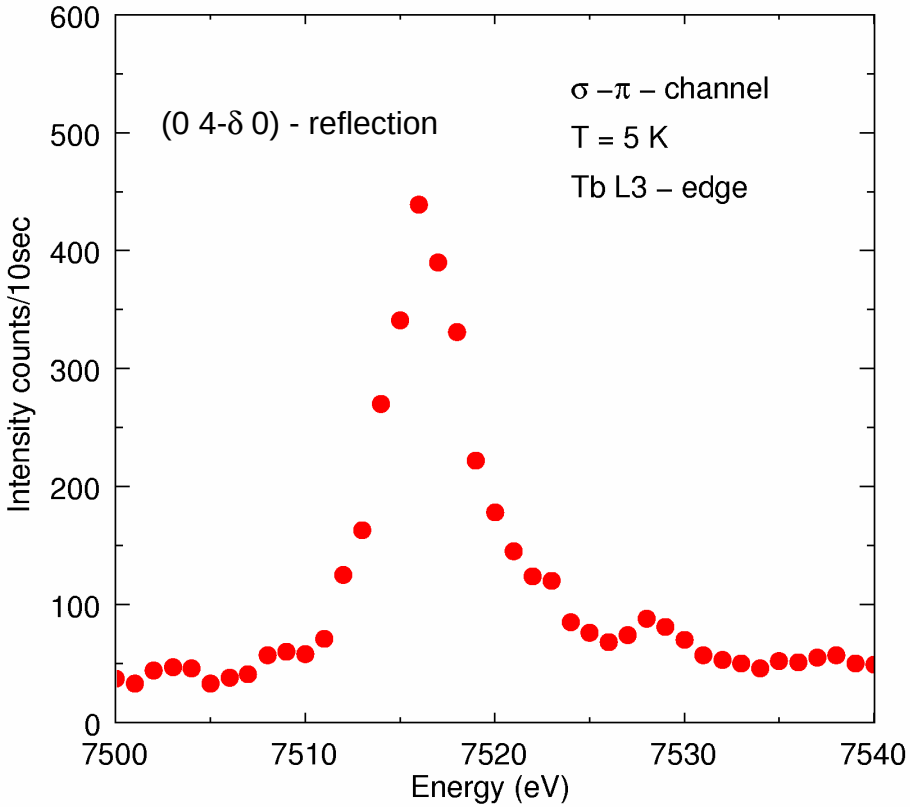

Summary of beamline features

- Energy variation:
  - Large energy range: 2.4 keV – 50 keV
- Small beam focus
  - Beam size routinely (mirror): 145 x 40 μm^2
  - with Compound Refractive Lenses: 7 x 4 μm^2
- Effective higher harmonic suppression
  - High harmonic suppression in full energy range 2.4 – 24 keV
- Variable x-ray polarization
  - Fully variable incident polarization in energy range 3.4 – 12 keV
  - Determination of scattered polarization states
- Psi-diffractometer
  - Open χ-circle
  - Quasi-simultaneous use of area and point detector
- Heavy Load Diffractometer
  - Horizontal 6-circle diffractometer
  - 650 kg load maximum
- Special sample environments
  - Low temperature cryostats
  - High magnetic fields: 14T magnet, high pulsed fields

Schedule for beamline commissioning

- October 2009: First beam in first experimental hutch (EH1)
  Start of beamline commissioning
- November 2009: First experiments
- April 2010: Installation of mirrors
- June 2010: Installation of phase retarder setup
- July 2010: Delivery of heavy load diffractometer
- End 2010: Delivery of 14 T magnet

→ First experiments in November 2009 using Psi diffractometer (no focussing, no higher harmonic suppression)

→ First user experiments in second beamtime cycle 2010 (Aug. – Dec.)

Sector 6 Team:

Sonia Francoual	(Beamline scientist P09)
Dinesh Kumar Shukla	(Post Doc P09)
David Reuther	(Engineer P09)
Rainer Döring	(Technician P08/P09)
Kathrin Pflaum	(Engineer P08)
Oliver Seeck	(Beamline Scientist in Charge, P08)
Hermann Franz	(PETRA III Project leader experiments)